TÜBİTAK

Turkish Journal of Agriculture and Forestry

http://journals.tubitak.gov.tr/agriculture/

Research Article

Turk J Agric For
(2021) 45: 91-101

doi:10.3906/tar-2001-79

The potential of Göktürk 2 satellite images for mapping burnt forest areas

Murat KURUCA, Dilek KÜÇÜK MATCI*, Uğur AVDAN
Research Institute of Earth and Space Sciences, Eskişehir Technical University, Eskişehir, Turkey

Received: 23.01.2020 • **Accepted/Published Online:** 01.10.2020 • **Final Version:** 10.02.2021

Abstract: Using remotely sensed data to identify burnt forest areas produces fast, economical, and highly accurate results. Accordingly, in this study we investigate the capabilities of Göktürk-2, Turkey's national satellite, for mapping burnt forest areas. We compare our results with those obtained from Landsat-8 and Worldview-2 satellite images, which are frequently used for mapping burnt areas. The capabilities of the satellites are compared, in terms of detecting burnt forest areas, using support vector machine (SVM) and rotation forest (RF) classification, which are advanced methods.-According to the results of the accuracy analysis, SVM classification gives similar kappa statistics and overall accuracy for Göktürk-2 and Landsat-8 images, while the performance of Worldview-2 shows greater general accuracy. Although there is no significant difference between the two classification methods forLandsat-8 images, SVM gives better results than RF for both Göktürk-2 and Worldview-2. The results of our study show that Göktürk-2 images are an effective source for mapping burnt forest areas.

Key words: Göktürk-2, mapping burnt forest area, object-based image analysis, rotation forest, support vector machine

1. Introduction

Forest fires are among the most important factors affecting the continuation of the existing ecosystem and greenhouse gas emissions. Mapping burnt areas is critical for fire extinguishing operations. Information about burnt surface area is important for assessing the effects of forest fires (Ling et al., 2015). Remote sensing is increasingly used as the main source of land cover information (Kramer, 2002; Foody and Mathur, 2004). Significant advances in satellite technology provide land cover information at spatial, temporal, spectral, and radiometric resolutions, covering a wide range of land uses (Anthony et al., 2007).

Mapping burnt forest areas using satellite imagery is an active subject of study. Some of the images used for this purpose come from the Worldview-2 satellite, the world's first high-resolution observation satellite with 8 spectral bands, which was launched in October 2009. Worldview-2 typically revisits a place on earth every 1.1 days and provides both 0.46 m panchromatic and 1.84 m multispectral resolution (Wu et al., 2015; Meng et al., 2017). The Landsat-8 satellite is also used for mapping burnt forest areas (Schroeder et al., 2016; Vhengani et al., 2015; Quintano et al., 2018); in the literature studies utilizing images obtained from Landsat-8 are the most frequently encountered (Fitriana et al., 2018; Long et al., 2019). In this study, the final satellite used for mapping burnt forest areas is Göktürk-2. This Turkish reconnaissance satellite, designed and developed by TÜBİTAK UZAY and integrated with TAI, was launched on December 18, 2012 from the Jiuquan Launch Base in China. The satellite weighs 409 kg and has a resolution of 2.5 m. It is the first satellite built for this purpose in the history of the Turkish Republic (Atak et al., 2015; Teke, 2016).

Support vector machine (SVM) classification is a supervised learning algorithm based on statistical learning theory (Cortes and Vapnik, 1995). It is used in many fields such as handwriting, character and signature recognition, and data mining (Cortes and Vapnik, 1995; Joachims, 1998). SVM is frequently used in satellite image processing (Huang et al., 2002; Bazi and Melgani, 2006; Bruzzone et al., 2006; Jiménez-Muñoz et al., 2009; Mountrakis et al., 2011; Myint et al., 2011; Gürcan et al., 2016). Conventional methods are insufficient to classify satellite images with similar spectral properties and nonhomogeneous, complex structures (Miller and Yool, 2002; Barbosa et al., 1999; Bayburt, 2009). In order to solve this problem, in recent years methods with multiple classifiers, instead of single classifiers, have been used; the most preferred among these are ensemble learning algorithms known as boosting, bagging, and random forest (Malinverni et al., 2011; Ghosh and Joshi, 2014). Presently, rotation forest (RF) classification has had

* Correspondence: dkmatci@anadolu.edu.tr

limited testing, as it is a new ensemble learning algorithm based on recreating a dataset using principal component analysis (Rodriguez et al., 2006; Kavzoğlu and Çölkesen, 2010).

The main aim of the study is to demonstrate the object-oriented classification performance for burnt forest areas using images from the Göktürk-2 satellite. Automatic mapping of burnt forest is done using the advanced classification methods SVM and RF. The second aim is to compare the results from the Göktürk-2 satellite with Landsat-8 and Worldview-2 satellite images. The final aim is to test the performances of SVM and RF, two supervised classification methods that provide high-accuracy results in other fields covered in the literature, for mapping burnt forest areas. For this purpose, the Antalya region, which has a first degree fire risk according to the Foresters' Association of Turkey (TOD)[1] was selected.

2. Materials and methods

2.1. Satellite data

Images sensed remotely after June 2016 from theGöktürk-2, Landsat-8, and Worldview-2 satellites were used for the detection of burnt forest areas. The band information of the satellites is given in Table 1.

Göktürk-2 has 5 bands: PAN, red, green, blue, and NIR. The true color band combination is 1, 2, and 3[2]. The

[1] Republic of Turkey Ministry of Agriculture and Forestry General Directorate of Forestry (2019). Title of resource [online]. Website https://www.ogm.gov.tr/lang/en/sitepages/ogm/ogmdefault.aspx [accessed 26 August 2019].

[2] GISAT (2019). Göktürk-2 [online]. Website http://www.gisat.cz/content/en/satellite-data/supplied-data/high-resolution/satelite/goektuerk-2 [accessed 29 August 2019].

Table 1. The characteristics of the spectral bands used of satellites [Abbreviations of spectral regions: B (blue), G (green), R (red), Y (yellow), NIR (near infrared), SWIR (short wave infrared)].

Satellite	Spectral band	Spectral region	Bandwidth (μm)	Spatial resolution (m)
Göktürk-2	1	B	0.45–0.52	5
	2	G	0.52–0.6	5
	3	R	0.63–0.69	5
	4	NIR	0.76–0.9	5
	5	PAN	0.42–0.75	2.5
Landsat-8 (OLI: Operational Land Imager)[1]	1	Coastal	0.435–0.451	30
	2	B	0.452–0.512	30
	3	G	0.533–0.590	30
	4	R	0.636–0.673	30
	5	NIR	0.851–0.879	30
	6	SWIR-1	1566–1651	30
	7	SWIR-2	2107–2294	30
	8	PAN	0.503–0.676	15
Worldview-2 (The WorldView-2 sensor)[2]	1	Coastal	0.400–0.450	1.85
	2	B	0.450–0.510	1.85
	3	G	0.510–0.580	1.85
	4	Y	0.585–0.625	1.85
	5	R	0.630–0.690	1.85
	6	Red edge	0.705–0.745	1.85
	7	NIR-1	0.770–0.895	1.85
	8	NIR-2	0.860–1040	1.85
	9	PAN	0.450–0.800	0.46

[1] Satellite Imaging Corporation (2020a). LANDSAT 8 Satellite Sensor (15m) [online]. Website https://www.satimagingcorp.com/satellite-sensors/other-satellite-sensors/landsat-8/ [10 January 2020].

[2] Satellite Imaging Corporation (2020b). WorldView-2 Satellite Sensor (0.46m) [online]. Website https://www.satimagingcorp.com/satellite-sensors/worldview-2/ [10 January 2020].

satellite image used in the study, dated 02.07.2016, was obtained from the Turkish Air Force Satellite Battalion. Göktürk-2 data belong to the General Staff, and all rights are reserved by the General Staff. Many academic studies use Göktürk-2 satellite images for topics such as land use, land cover, and automatic detail extraction (Gürcan et al., 2016; Teke and Yardımcı, 2016; Akar and Görmüş, 2019).

Landsat-8 provides images in the thermal-infrared, short-wave-infrared, near-infrared, and visible wavelength ranges. The Landsat-8 satellite provides data with a spatial resolution of 15 m to 100 m according to the spectral value[3]. The satellite image from 09.08.2016 was used in this study.

Worldview-2 was the first and only observation satellite with 8 multispectral bands until Worldview-3 was launched (Qian et al., 2015). The image from 14.07.2016 was used for the detection of burnt forest areas in this study. No other fires were reported between the date of the fire under study and the dates of the satellite images.

2.2. Study area

The Kumluca and Adrasan forest fires occurred in Antalya between the 24th and 27th of June 2016, and more than 500 ha were burned. Forest animals perished, and the fire threatened private homes and caused material losses[4]. A Google Earth image of the region is given in Figure 1.

The region where the fires occurred is located on the Teke peninsula in the Antalya area of the Mediterranean region. Geographically located in the middle belt, the region is known for its warm climate. The dominant forest type in the Mediterranean region is *Pinus brutia* (red pine), along with *Ceratonia siliqua*, *Quercus coccifera*, *Olea europea*, *Myrtus communis*, and *Pistacia terebinthus*, which are maquis plants that grow below 700 m. There are also moisture-loving species such as *Platanus orientalis*, *Nerium oleander*, and *Vitex agnus-castus* (Municipality, 2020)[5].

2.3. Methods

The method applied for mapping burnt areas consists of 6 steps: image fusion, segmentation, calculation of indexes,

[3] Science NL. Landsat 8. [accessed 26 August 2019].

[4] Orman Fakülteliler Derneği (ORFAMDER) (2019). Kumluca ve Adrasan Yangınları (in Turkish) [online]. Website https://www.orfamder.org/haberler/kumluca-ve-adrasan-yanginlari/ [26 August 2019].

[5] Kumluca Municipality (2020). Geography [online]. Website http://www.kumluca-bld.gov.tr/19/COGRAFYA.html [accessed 26 April 2020].

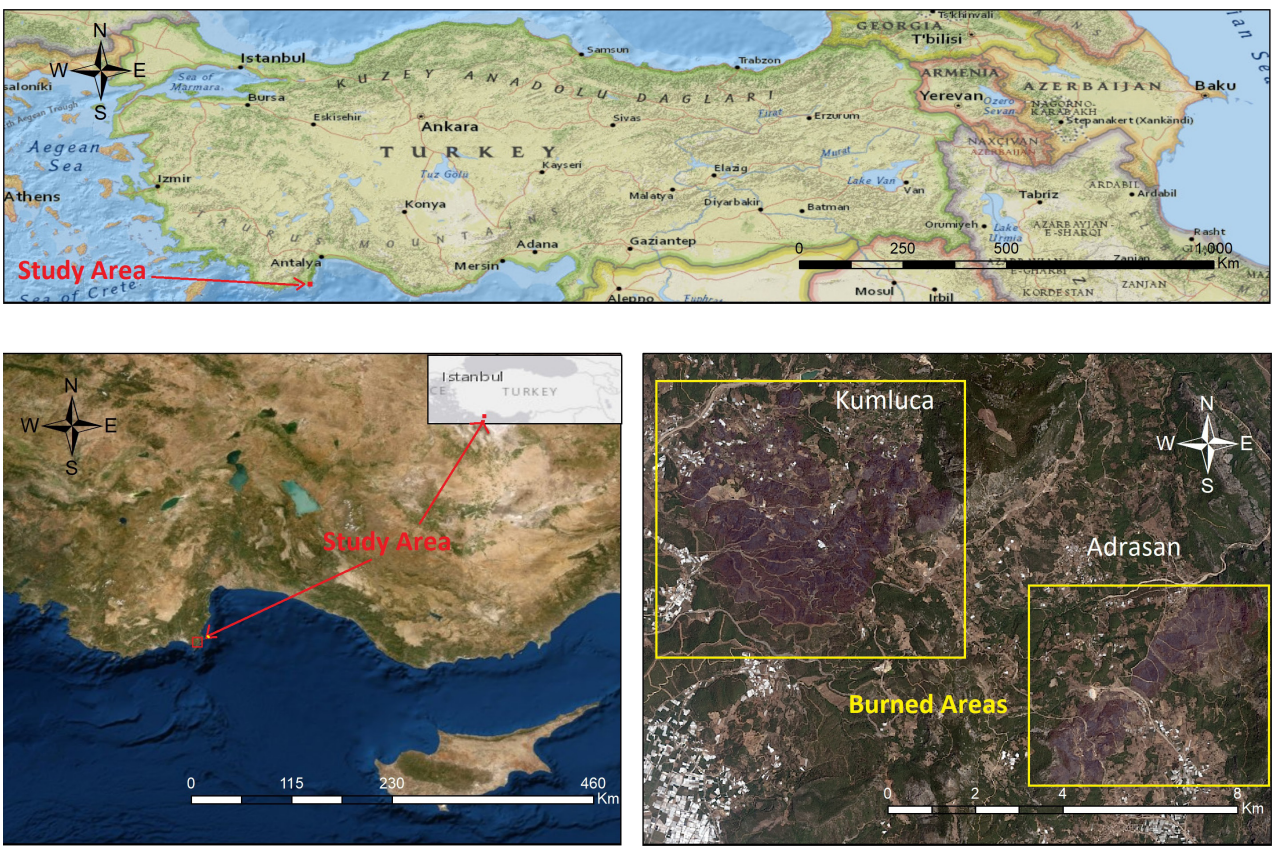

Figure 1.Kumluca and Adrasan fire areas.

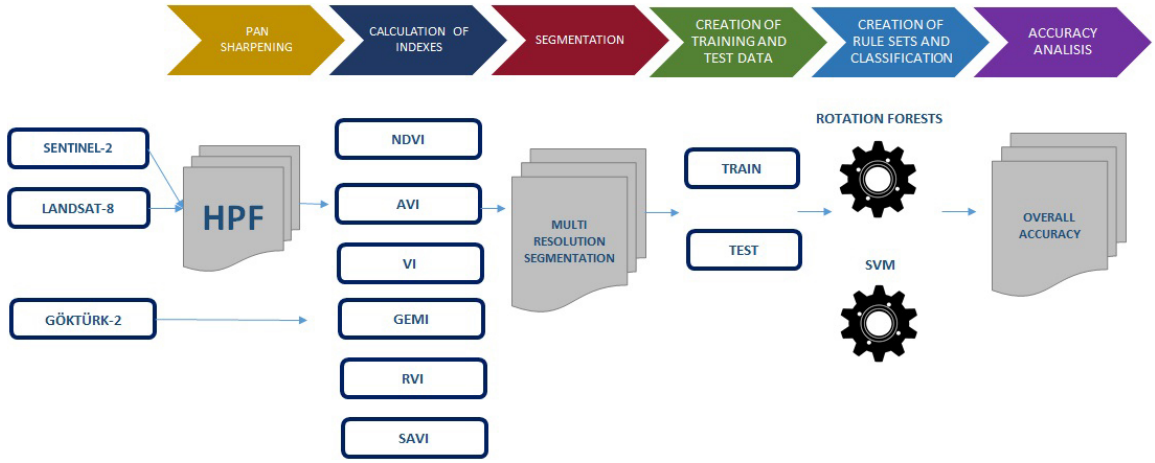

Figure 2. Flowchart of the methodology used for burnt area classification.

preparation of training and test data, classification of data by forming classifier models, and accuracy analysis (Figure 2).

The classification process is carried out using images from Göktürk-2, Landsat-8, and Worldview-2 in order to detect burnt areas resulting from the forest fires that occurred in Adrasan and Kumluca (Antalya) in June 2016. To perform image segmentation, the normalized difference vegetation index (NDVI), relative vegetation index (RVI), soil-adjusted vegetation index (SAVI), global environmental monitoring index (GEMI), Ashburn vegetation index (AVI), vegetation index (VI), and normalized burned ratio (NBR) are used. The RF and SVM processes, both object-based advanced classification techniques, are applied to the dataset to detect burnt areas. The process results in two classes, burnt areas and unburnt areas. Accuracy analysis is applied to the classes obtained.

2.3.1. Preparing images and pan-sharpening

In the first step of the study, band combination and pan-sharpening were applied to the Landsat-8 and Worldview-2 images, while band combination was applied to the Göktürk-2 image. In the image fusion step, fusion of the panchromatic and spectral bands was achieved using the HPF resolution merge algorithm, which combines high-resolution panchromatic data with lower resolution multispectral data, resulting in an output with both excellent detail and a realistic representation of the original multispectral scene colors (Gangkofner et al., 2007; Zheng et al., 2007; Zhang and Mishra, 2012).

2.3.2. Segmentation

The best settings for segmentation parameters are numerous and generally determined through a combination of trial-and-error, fault, and experience. Even when images are identical, the same best settings may not work for both. Color/shape, density/smoothness, and scale criteria are the three most common parameters used in segmentation (Sunar, 2018). At this stage, the segmentation was performed with eCognition Developer (v. 9.0). Using this function, the optimum parameter values were quickly determined for a small area of study shown in Table 2.

Segmentation was performed using these determined parameters, and indices and objects were created from pixels.

2.3.3. Determination of indices

For determination of objects during segmentation, the band values were subject to a number of formulation processes to obtain proportions. Accordingly, in the second stage of the study, the literature was searched, and indices used in other studies were identified (Ashburn, 1979; Tucker, 1979; Huete, 1988; Pinty and Verstraete, 1992; Blackburn, 1998; Sunar, 2018) (Table 3).

As seen in Table 3, NBR and NBR 2 indices were calculated using the Landsat-8 image, unlike other satellite images. These indexes are frequently used in the literature to map burnt areas. Due to the absence of SWIR bands in the Worldview-2 and Göktürk satellites, these indices could not be calculated for images from these two satellites. However, these indices were used to examine whether these bands in the Landsat-8 satellite provide an advantage in mapping burnt areas. Calculations for Landsat-8 images were performed both with and without these indices, and the results were compared.

2.3.4. Creation of training and test data

In the fourth stage, the test and training regions used for classification were determined. We used the Kumluca region for the training data (8701 samples) and the Adrasan region for the test data. The selected test and training areas are geographically very close, with the same physiographic and climatic features. They show high similarity in terms of vegetation, and only two days elapsed between the fires in each region.

Table 2. Segmentation parameter values.

Satellite	Scale parameter	Shape parameter	Density parameter
Göktürk-2	80	0.3	0.7
Landsat-8	100	0.4	0.6
Worldview-2	120	0.3	0.7

Table 3. Classification indices.

Satellites	Derived indices	equation
Göktürk-2	Normalized difference vegetation index (NDVI) (Trucker, 1979)	(B4–B3)/(B4+B3)
	Relative vegetation index (RVI) (Blackburn, 1998)	(B4/B3)
	Soil-adjusted vegetation index (SAVI) (Huete, 1988)	(B4–B3)/(B4 + B3 + L) × (1 + L); L = 0.5
	Global environmental monitoring index (GEMI) (Pinty and Verstraete, 1992)	GEMI = γ(1−0,25γ) −((B3−0,125))/((1−B3)) γ = [2(B4²–B3²)+ 1,5B4+0,5B3]/((B4+B3+0,5))
	Ashburn vegetation index (AVI) (Ashburn, 1979)	2XB4–B3
	Vegetation index (VI) (Gitelson et al. 2002)	(B2–B3)/(B2+B3)
Landsat-8	Normalized difference vegetation index (NDVI)	(B5–B4)/(B5 + B4)
	Relative vegetation index (RVI)	(B5/B4)
	Soil-adjusted vegetation index (SAVI)	(B5–B4)/(B5 + B4 + L) × (1 + L); L = 0.5
	Global environmental monitoring index (GEMI)	GEMI = γ(1−0,25γ)−((B4−0,125))/((1−B4)) γ = [2(B5²–B4²)+ 1,5B5+0,5B4]/((B5+B4+0,5))
	Ashburn vegetation index (AVI)	2XB5–B4
	Vegetation index (VI)	(B3–B4)/(B3+B4)
Worldview-2	Normalized difference vegetation index (NDVI)	(B6–B5)/(B6+B5)
	Relative vegetation index (RVI)	(B6/B5)
	Soil-adjusted vegetation index (SAVI)	(B6–B5)/(B6 + B5 + L) × (1 + L); L = 0.5
	Global environmental monitoring index (GEMI)	GEMI = γ(1−0,25γ)−((B5−0,125))/((1−B5)) Γ = [2(B6²–B5²)+ 1,5B6+0,5B5]/((B6+B5+0,5))
	Ashburn vegetation index (AVI)	2XB6–B5
	Vegetation index (VI)	(B3–B5)/(B3+B5)

There are some basic principles for the selection of training examples when applying pixel-based classification (Van Niel et al., 2005; Foody et al., 2006). The number of object-based training samples, however, is usually determined based on researcher experience (Qian et al., 2015).

2.3.5. Creating classification models and classification

One method used to detect burnt and unburnt areas in this study is the SVM classifier, which can effectively solve both linear and nonlinear classification problems. Large nonlinear separable datasets can be separated linearly using the kernel function (Vapnik, 1995). The radial basis function (RBF) kernel, the sigmoid kernel, and the polynomial kernel are the three most commonly used kernel functions[6] (Gunn, 1998; Han et al., 2012). In this study, the most common Gaussian RBF kernel is used (Melgani and Bruzzone, 2004; Waske and Benediktsson, 2007). In order to classify using the Gaussian RBF kernel, two values must be specified by the user; the C parameter, which is a regulation parameter for incorrect classification errors, and the hyper parameter, γ, which controls the trade-off between error due to bias and variance in a model (Hsu et al., 2003). As the value of C increases the model overfits, and as the value of C decreases the model underfits. As the value of γ increases the model overfits, and as the value of γ decreases the model underfits. In this study, a trial-and-error method is used to find the appropriate values of these parameters, then training sets are created with the determined parameters (Table 4).

The rotation forest (RF) method is successful at generating classifier ensembles based on feature extraction

[6] Lin H-T, Lin C-J (2003). A study on sigmoid kernels for SVM and the training of non-PSD kernels by SMO-type methods (unpublished manuscript).

Table 4. SVM classification parameter values.

Satellite	SVM	
	C	γ
Göktürk-2	1.0	$1.0e^{-12}$
Landsat-8	1000	$1.0e^{-3}$
Worldview-2	1000	$1.0e^{-12}$

(Rodriguez et al., 2006). The purpose of this method is to ensure the individual accuracy and diversity of the members in a classifier ensemble (Xia et al., 2014). The RF algorithm for classification is a linear transformation method which provides a new field of performance within the classifier ensemble (Liu and Huang, 2008). The algorithm uses many tree algorithms as the basic working principle, similar to random forest algorithm, but differs in that it uses different feature fields, such as principal component analysis (PCA), to create a dataset. Many decision trees are produced using the training datasets identified by the field. Using the RF algorithm, the training dataset is subdivided into decision trees, and the selected property field from each subset is extracted as an attribute (Liu and Huang, 2008). Because of this feature, the RF algorithm generally gives better classification accuracy than the random forest algorithm (Rodriguez et al., 2006). The parameters of the algorithm used in this study are given in Table 5.

2.4. Accuracy analysis

In the last stage of the study, control points were created and accuracy analysis was performed. Accuracy analysis determines the accuracy of the classes formed by the classification process and is a control method based on the principle of statistical comparison of the map or terrain data used as reference with the pixel values classified. The most preferred of these methods are general, user, and manufacturer accuracy (Yan et al., 2006).

The number of control points required for two classifications is found according to two-term probability theory (Snedecor and Cochran, 1967; Aronoff, 1982; Lucas et al., 1994). According to this theory, at least 319 control points are needed for reliable accuracy, with an accuracy expectation of 85% and an acceptable error of 4%; 350 control points are used in this study.

In this study two classes, burnt and unburnt, were determined. Using two-term probability theory, the number of control points needed was calculated (Snedecor and Cochran, 1967). According to the theory:

$$N = \frac{Z^2 xpxq}{E^2} \quad (1)$$

where

Table 5. RF classification parameter values.

Göktürk-2	Classifier	Random tree			
		K	M	V	S
		0	1	0.001	1
	Projection filter	Random projection			
		N	R	D	
		10	95	Sparse 1	
Landsat-8	Classifier	Random forest			
		K	M	V	S
		0	1	0.001	1
	Projection filter	Random projection			
		N	R	D	
		10	42	Sparse 1	
Worldview-2	Classifier	J48			
		C		M	
		0.25		2	
	Projection filter	Random projection			
		N	R	D	
		10	95	Sparse 1	

Random Tree/Forest; K: number of attributes to randomly investigate, M: set minimum number of instances per leaf, V: set minimum numeric class variance proportion of train variance for split, and S: seed for random number generator.
Random Projection; N: the number of dimensions (attributes) the data should be reduced to, R: the random seed for the random number generator used for calculating the random matrix, D: the distribution to use for calculating the random matrix. J48; C: set confidence threshold for pruning, and M: set minimum number of instances per leaf.

N: number of samples needed,

Z: value from the Z table for the specified confidence level,

p: expected accuracy,

q = 100 – p,

E: acceptable error (Fitzpatrick-Lins, 1981).

3. Results and discussion

When the results are analyzed, it can be seen that almost all the burnt areas were detected automatically (Figures 3 and 4). Accuracy analysis of SVM and RF shows that both classifications are suitable methods for detecting burnt areas.

The accuracy results were analyzed for reliability of classification, as shown in Table 6. When the two classifications are compared, it can be seen that SVM is more successful than RF. In conclusion, images from all three satellites are suitable for such studies.

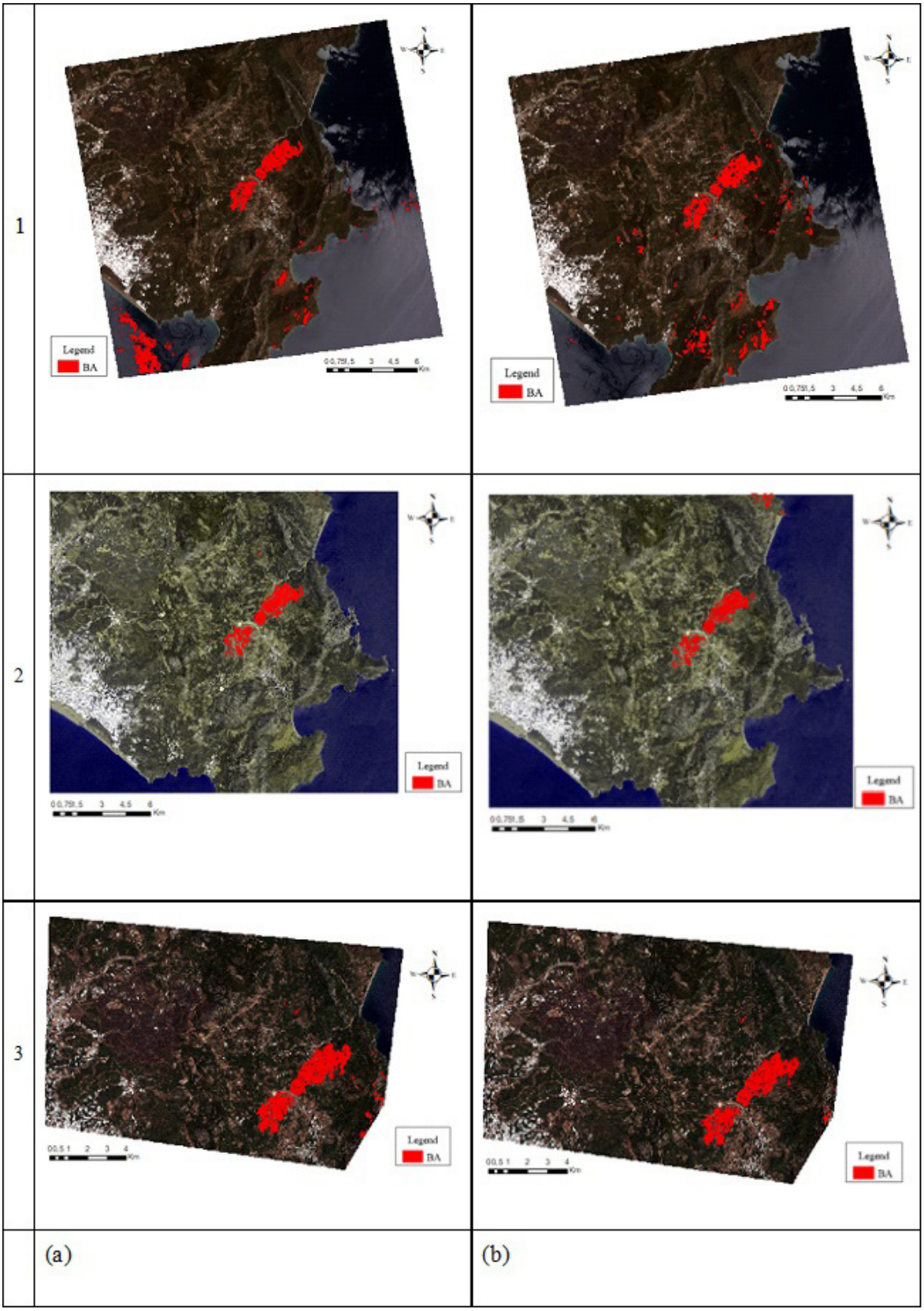

Figure 3. Screenshot of (a) SVM and (b) RF classifications of (1) Göktürk-2, (2) Landsat-8, and (3) Worldview-2 satellites.

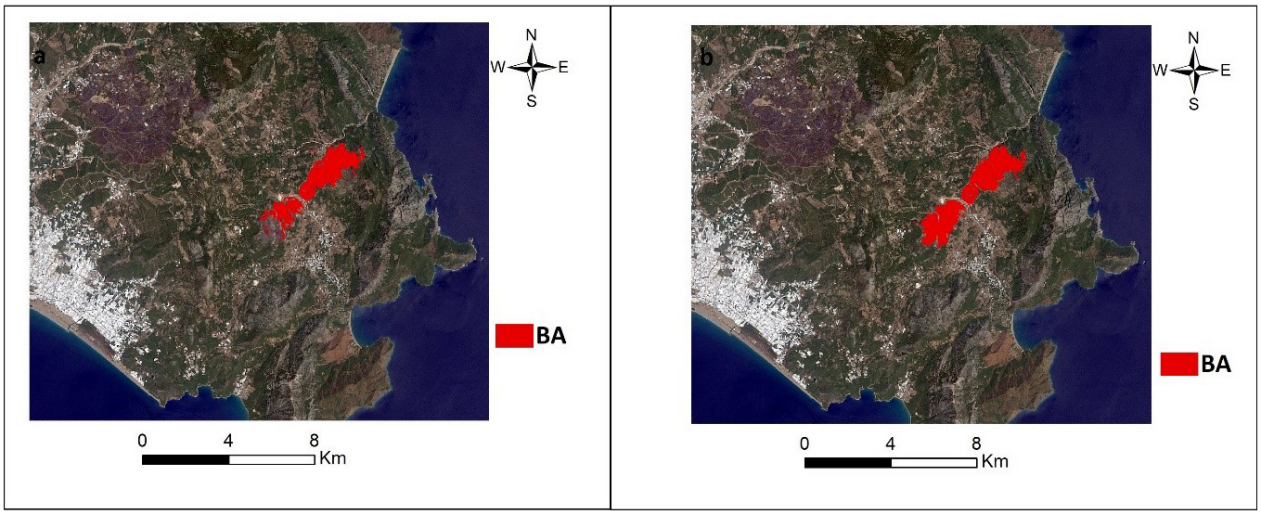

Figure 4. Result maps of Landsat-8 with new indices (a) SVM, and (b) RF classifications.

Table 6. Accuracy analysis results.

Satellite	Method	User accuracy	Producer accuracy	Omission error	Commission error	Kappa	Overall accuracy
Göktürk-2	SVM	86.93	78.70	11.83	13.07	0.68	0.84
	RF	79.08	79.83	20.92	20.92	0.63	0.82
Landsat-8	SVM	75.46	89.78	29.20	24.54	0.69	0.85
	RF	76.07	89.21	28.06	23.93	0.69	0.85
Landsat-8 with NBR and NBR-2	SVM	78	94	22	4	0.756	0.88
	RF	92	94	8	94	0.877	0.94
Worldview-2	SVM	93.38	94.63	6.71	6.62	0.90	0.95
	RF	86.75	97.76	14.93	13.25	0.86	0.93

When the result maps are examined, areas other than the areas burned in 2016 are classified as burnt areas. Some of these misclassified areas are as presumed to be old burnt areas. Since the aim of the study isto identify the areas burnt in June 2016, the old burnt areas are considered misclassified, although the areas did burn, and the classification is considered incorrect since the data are outside the search field. This reduces the accuracy of the study.

When the literature is investigated, the NBR index and NBR2 index are generally used (Loboda et al., 2007; Roy et al., 2006; Epting et al., 2005; Çölkesen et al., 2015). In this study, these indices are only used for Landsat-8, since there are no SWIR band values in the Göktürk-2 or Worldview-2 images. In order to evaluate the advantages of these indices for the detection of burnt areas, Landsat-8 data is classified together with these index values. The result maps of the Landsat-8 image classification with the NBR and NBR 2 indices are given in Figure 4. When the results obtained using NBR and NBR 2 indices are examined, the overall accuracy rates increase for both SVM and RF, when NBR and NBR2 index values are used along with the other indices. This provides a 10% increase, particularly as a result of the classification made with random forests.

4. Conclusion

In this study, images from the Göktürk-2 satellite, which have not previously been used for this purpose, are used to identify burnt forest areas. We conduct an analysis of the results obtained using two advanced classification methods: rotation forest and support vector machine classifiers. We compare our results with Landsat-8 and Worldview-2 images, which are frequently used in the literature.

When the classification results are examined, the performance of all three satellites is good. Since the resolution of the Worldview-2 satellite is higher than the other satellites, it gives the best results. Considering that

the services provided by Göktürk-2 and Landsat-8 are free, the use of these satellites is preferable due to their satisfactory performance in such studies.

Göktürk-2, Turkey's national satellite, gives good results for such studies, yet it is rarely used in the current literature. Increasing the use of Göktürk-2 for remote sensing studies may support the future design of satellites for civilian, and not just military, needs.

The application of advanced techniques such as support vector machine and rotation forest classification, and the use of data mining in classification processes, are methods of remote sensing that provide more accurate classification in less time.

Acknowledgments

This study was produced from a master's thesis (thesis no.: 535677;Locating burned forest areas with satellite images) written by Murat KURUCA under the supervision of Assoc. Prof. Uğur Avdan.

The authors would like to thank the Turkish Air Force for providing Göktürk-2 satellite imagery and Mr. Bilal KORKMAZ for his support.

References

Akar Ö, Görmüş ET (2019). Göktürk-2 ve Hyperion EO-1 uydu görüntülerinden rastgele orman sınıflandırıcısı ve destek vektör makineleri ile arazi kullanım haritalarının üretilmesi. Geomatik 4 (1): 68-81 (in Turkish). doi: 10.29128/geomatik.476668

Anthony G, Greg H, Tshilidzi M (2007). Classification of images using support vector machines. arXiv preprint. arXiv: 07093967.

Aronoff S (1982). Classification accuracy: a user approach. Photogrammetric Engineering and Remote Sensing 48:1299-1307.

Ashburn P (1979). The vegetative index number and crop identification. Johnson Space Center Proceedings of Technical Sessions, Vol. 1. Houston, TX, USA: NASA Johnson Space Center.

Atak VO, Erdoğan M, Yılmaz A (2015). Göktürk-2 uydu görüntü testleri. Harita Dergisi 81: 18-33 (in Turkish)

Barbosa PM, Stroppiana D, Grégoire J-M, Pereira JMC (1999b). An assessment of vegetation fire in Africa (1981–1991): burned areas, burned biomass, and atmospheric emissions. Global Biogeochemical Cycles 13: 933-950.

Bayburt S (2009). Uydu görüntülerinin piksel ve nesne tabanlı sınıflandırma sonuçlarının karşılaştırılması (Doğu Trakya Bölgesi örneği). MSc, İstanbul Technical University, İstanbul, Turkey.

Bazi Y, Melgani F (2006). Toward an optimal SVM classification system for hyperspectral remote sensing images. IEEE Transactions on Geoscience and Remote 44: 3374-3385.

Blackburn GA (1998). Spectral indices for estimating photosynthetic pigment concentrations: a test using senescent tree leaves. International Journal of Remote Sensing 19: 657-675.

Bruzzone L, Chi M, Marconcini M (2006). A novel transductive SVM for semisupervised classification of remote-sensing images. IEEE Transactions on Geoscience and Remote 44:3363-3373.

Çölkesen İ, Yomralıoğlu T, Kavzoğlu T (2015).Obje tabanlı sınıflandırmada bölgeleme esasına dayalı ölçek parametresi tespiti: WorldView-2 uydu görüntüsü örneği. Harita Dergisi 154: 9-18 (in Turkish).

Cortes C, Vapnik V (1995). Support-vector networks. Machine Learning 20: 273-297.

Epting J, Verbyla D, Sorbel B (2005). Evaluation of remotely sensed indices for assessing burn severity in interior Alaska using Landsat TM and ETM+. Remote Sensing of Environment 96: 328-339.

Fitriana HL, Prasasti I, Khomarudin MR (2018). Mapping burned areas from landsat-8 imageries on mountainous region using reflectance changes. MATEC Web of Conferences 229. doi: 10.1051/matecconf/201822904012

Fitzpatrick-Lins K (1981). Comparison of sampling procedures and data analysis for a land-use and land-cover map. Photogrammetric Engineering and Remote Sensing 47: 343-351.

Foody GM, Mathur A (2004). A relative evaluation of multiclass image classification by support vector machines. IEEE Transactions on Geoscience and Remote 42: 1335-1343.

Foody GM, Mathur A, Sanchez-Hernandez C, Boyd DS (2006). Training set size requirements for the classification of a specific class. Remote Sensing of Environment 104: 1-14.

Gangkofner UG, Pradhan PS, Holcomb DW (2007). Optimizing the high-pass filter addition technique for image fusion. Photogrammetric Engineering & Remote Sensing 73: 1107-1118.

Ghosh A, Joshi PK (2014). A comparison of selected classification algorithms for mapping bamboo patches in lower Gangetic plains using very high resolution WorldView 2 imagery. International Journal of Applied Earth Observation and Geoinformation 26: 298-311.

Gitelson AA, Kaufman YJ, Stark R, Rundquist D (2002). Novel algorithms for remote estimation of vegetation fraction. Remote sensing of Environment 80: 76-87.

Gunn SR (1998). Support vector machines for classification and regression. ISIS technical report 14: 5-16.

Gürcan İ, Teke M, Leloğlu UM (2016). Land use/land cover classification for Göktürk-2 satellite. In: 24th Signal Processing and Communication Application Conference (SIU); Zonguldak, Turkey. pp. 2097-2100.

Han S, Qubo C, Meng H (2012). Parameter selection in SVM with RBF kernel function. In: World Automation Congress 2012; Puerto Vallarta, Mexico. pp. 1-4.

Hsu C-W, Chang C-C, Lin C-J (2003). A practical guide to support vector classification. Taipei City, Taiwan: National Taiwan University.

Huang C, Davis L, Townshend J (2002). An assessment of support vector machines for land cover classification. International Journal of Remote Sensing 23: 725-749.

Huete AR (1988). A soil-adjusted vegetation index (SAVI). Remote Sensing of Environment 25: 295-309.

Jiménez-Muñoz J, Sobrino J, Plaza A, Guanter L, Moreno J et al. (2009). Comparison between fractional vegetation cover retrievals from vegetation indices and spectral mixture analysis: case study of PROBA/CHRIS data over an agricultural area. Sensors 9: 768-793.

Joachims T (1998). Text categorization with support vector machines: Learning with many relevant features. In: European conference on machine learning. Springer, pp 137-142.

Kavzoğlu T, Çölkesen İ (2010). Destek vector makineleri ile uydu görüntülerinin sınıflandırılmasında kernel fonksiyonlarının etkilerinin incelenmesi. Harita Dergisi 144: 73-82 (in Turkish).

Kramer HJ (2002). Observation of the Earth and its Environment: Survey of Missions and Sensors. Berlin, Germany: Springer Science & Business Media.

Ling F, Du Y, Zhang Y, Li X, Xiao F (2015). Burned-area mapping at the subpixel scale with MODIS images. IEEE Geoscience and Remote Sensing Letters 12: 1963-1967.

Liu K-H, Huang D-S (2008). Cancer classification using rotation forest. Computers in Biology and Medicine 38: 601-610.

Loboda T, O'neal K, Csiszar I (2007). Regionally adaptable dNBR-based algorithm for burned area mapping from MODIS data. Remote Sensing of Environment 109: 429-442.

Long T, Zhang Z, He G, Jiao W, Tang C et al. (2019). 30 m resolution global annual burned area mapping based on landsat images and Google Earth Engine. Remote Sensing 11:489.

Lucas I, Janssen F, van der Wel F (1994). Accuracy assessment of satellite derived land-cover data: a review. Photogrammetric Engineering and Remote Sensing 60: 426-479.

Malinverni ES, Tassetti AN, Mancini A, Zingaretti P, Frontoni E et al. (2011). Hybrid object-based approach for land use/land cover mapping using high spatial resolution imagery. International Journal of Geographical Information Science 25: 1025-1043.

Melgani F, Bruzzone L (2004). Classification of hyperspectral remote sensing images with support vector machines. IEEE Transactions on Geoscience and Remote 42: 1778-1790.

Meng R, Wu J, Schwager KL, Zhao F, Dennison PE (2017). Using high spatial resolution satellite imagery to map forest burn severity across spatial scales in a Pine Barrens ecosystem. Remote Sensing of Environment 191: 95-109.

Miller JD, Yool SR (2002). Mapping forest post-fire canopy consumption in several overstory types using multi-temporal Landsat TM and ETM data. Remote sensing of Environment 82: 481-96.

Mountrakis G, Im J, Ogole C (2011). Support vector machines in remote sensing: a review. ISPRS Journal of Photogrammetry and Remote Sensing 66: 247-259.

Myint SW, Gober P, Brazel A, Grossman-Clarke S, Weng Q (2011). Per-pixel vs. object-based classification of urban land cover extraction using high spatial resolution imagery. Remote Sensing of Environment 115: 1145-1161.

Pinty B, Verstraete M (1992). GEMI: a non-linear index to monitor global vegetation from satellites. Vegetatio 101: 15-20.

Qian Y, Zhou W, Yan J, Li W, Han L (2015). Comparing machine learning classifiers for object-based land cover classification using very high resolution imagery. Remote Sensing 7: 153-168.

Quintano, C, Fernández-Manso A,Fernández-Manso O (2018). Combination of Landsat and Sentinel-2 MSI data for initial assessing of burn severity. International Journal of Applied Earth Observation and Geoinformation 64: 221-25.

Rodriguez JJ, Kuncheva LI, Alonso CJ (2006). Rotation forest: A new classifier ensemble method. IEEE Transactions on Pattern Analysis and Machine Intelligence 28: 1619-1630.

Roy DP, Boschetti L, Trigg SN (2006). Remote sensing of fire severity: assessing the performance of the normalized burn ratio. IEEE Geoscience and Remote Sensing Letters 3: 112-116.

Schroeder W, Oliva P, Giglio L, Quayle B, Lorenz E (2016). Active fire detection using Landsat-8/OLI data. Remote sensing of Environment 185: 210-20.

Snedecor GW, Cochran WG (1967). Statistical Methods. Ames, IA, USA: Iowa State University Press.

Sunar F (2018). Digital Görüntü İşleme. Eskişehir, Turkey: Anadolu Üniversitesi Yayınları (in Turkish).

Teke M (2016). Satellite image processing workflow for RASAT and Göktürk-2. Journal of Aeronautics and Space Technologies 9: 1-13.

Tucker CJ (1979). Red and photographic infrared linear combinations for monitoring vegetation. Remote sensing of Environment 8: 127-150.

Van Niel TG, , McVicar TR, Datt B (2005). On the relationship between training sample size and data dimensionality: Monte Carlo analysis of broadband multi-temporal classification. Remote Sensing of Environment 98: 468-80.

Vapnik, Vladimir N(1995). The Nature of Statistical Learning Theory. New York, NY, USA: Springer. doi: 10.1007/978-1-4757-2440-0

Vhengani L, Frost P, Lai C, Booi N, Van den Dool R et al. (2015). Multitemporal burnt area mapping using Landsat 8: Merging multiple burnt area indices to highlight burnt areas. In: IEEE International Geoscience and Remote Sensing Symposium (IGARSS); Milan, Italy. pp. 4153-4156.

Waske B, Benediktsson JA (2007). Fusion of support vector machines for classification of multisensor data. IEEE Transactions on Geoscience and Remote 45: 3858-3866.

Wu Z, Middleton B, Hetzler R, Vogel J, Dye D (2015). Vegetation burn severity mapping using Landsat-8 and WorldView-2. Photogrammetric Engineering & Remote Sensing 81: 143-154.

Xia J, Chanussot J, Du P, He X (2014). Spectral–spatial classification for hyperspectral data using rotation forests with local feature extraction and Markov random fields. IEEE Transactions on Geoscience and Remote 53: 2532-2546.

Yan G, Mas JF, Maathuis B, Xiangmin Z, Van Dijk P (2006). Comparison of pixel-based and object-oriented image classification approaches—a case study in a coal fire area, Wuda, Inner Mongolia, China. International Journal of Remote Sensing 27: 4039-4055.

Zhang Y, Mishra RK (2012). A review and comparison of commercially available pan-sharpening techniques for high resolution satellite image fusion. In: IEEE International Geoscience and Remote Sensing Symposium; Munich, Germany. pp. 182-185.

Zheng Z, Li J, Ren J (2007). Discussion for technology ff HPF resolution merge using in Dali's remote sensing image. Yunnan Geographic Environment Research 20.